Lattice models of biological growth

David A. Young and Ellen M. Corey
Lawrence Livermore National Laboratory, University of California, Livermore, California 94550
(Received 20 February 1990)

We show that very simple iterative rules for the growth of cells on a two-dimensional lattice can simulate biological-growth phenomena realistically. We discuss random cellular automata models for the growth of fern gametophytes, branching fungi, and leaves, and for shape transformations useful in the study of biological variation and evolution. Although there are interesting analogies between biological and physical growth processes, we stress the uniqueness of biological automata behavior. The computer growth algorithms that successfully mimic observed growth behavior may be helpful in determining the underlying biochemical mechanisms of growth regulation.

I. INTRODUCTION

The field of pattern formation and fractal growth processes in physics has attracted much attention in recent years.[1-3] Some of the interest shown in this subject has surely been excited by the construction of complex and beautiful spatial patterns from very simple computer algorithms, as well as by the close match between the theoretical model results and observations of natural pattern formation phenomena. Physical pattern formation phenomena have many interesting analogies in biology, and it is worthwhile to apply the computational methods which have proven successful in physics to the more complex problems in biology.[4] In doing so, we hope to encourage a more quantitative approach to the study of biological growth and pattern formation.

Problems of biology are more difficult than problems of physics in the sense that the vast complexity of biological systems prevents us from describing the processes at work in any phenomenon in terms of simple equations. Although biological growth must involve the production, transport, and chemical transformation of biologically active molecules, the specific processes and their rates are unknown. This ignorance forces us to attack the problem of growth indirectly.

In this paper we use very simple random cellular automata to mimic biological growth in two dimensions. As in physical pattern formation, we assume that complex biological patterns are the result of iterating simple algorithms or rules. Our approach involves parametrization of growth rules, trial-and-error simulation of growth, and comparison with observed biological shapes and growth patterns. When simulations are found which match observed patterns, we assume that we have discovered a logical structure in the growth rules which is possessed by the actual biological process. We may then speculate on the biochemical processes underlying the successful growth rules. In the absence of detailed knowledge of the mechanisms, the plausibility of the model will be determined by its simplicity.

The growth rules lie at an intermediate level between the subcellular genetic-biochemical processes and the three-dimensional form of the whole organism: genes→growth rules→organism. Traditional discussions of developmental biology have always attempted to close the huge gap between the genes and the whole organism by rather vague speculation. Successful computer simulation of the growth process narrows this gap and allows us to make more intelligent guesses about the chain of causation from genes to organisms. Such theoretical work will be useful if it stimulates new experiments.

A better understanding of biological growth is a respectable goal by itself, but a broader objective would include the study of variation and evolution. A set of parametrized growth rules has limits to the parameter values which define the allowable shapes which can be produced by those rules. The shape variations created by random parameter (i.e., genetic) changes are then acted upon by environmental conditions (natural selection) to produce evolutionary change. Theoretical growth models might thus contribute to the understanding of evolution.

For physics, the study of biological growth is an opportunity to attack longstanding and intractable problems with the rigorous method of computer simulation and to open up a vast domain of natural phenomena to quantitative study. It is very likely that biological systems exhibit forms of collective behavior not seen in simpler physical systems.

II. GROWTH MODEL

A rigorous growth model might represent the growth of a three-dimensional object by means of modern numerical continuum-mechanics techniques. This would involve Lagrangian zoning of the growing tissue and a set of equations specifying the location and rate of synthesis of new cellular material, the resulting differential stresses developed within the tissue, and the plastic yielding of the tissue to produce a specific pattern of growth. Rezoning of the growing tissue would be required as the zones expanded and changed shape.

Such a program is unprofitable at present because it is computationally very expensive and because of our ignorance of the governing equations. Instead, we choose a much simpler scheme for two-dimensional growth. An

x-y rectangular grid is established in a box of predetermined size, typically 100×100 points. The grid spacing is set at 1. The grid points may be occupied or empty. An occupied point is a living "cell." These model "cells" are not to be confused with biological cells, but are simply the discretized points of a growing continuum. Biological tissue can grow either by cell division or cell enlargement, but this distinction is not made in the model. A model cell grows by division in one of the eight nearest-neighbor directions, as indicated in Fig. 1. In sliding growth,[5] a growing cell creates a new daughter cell which displaces a line of the existing neighbor cells by one lattice space in the direction of growth. Displacement stops when one of the displaced cells moves to an empty site. This is illustrated in Fig. 2. In accretion growth, new cells are placed only at empty sites. These are Eulerian, as opposed to Lagrangian, growth models.

Rules of growth of the cells are elaborated by specifying certain variables. In general, we allow growth by choosing the growing cell with a random number. If all cells are given equal probability, the growth is uniform. In nonuniform growth, the probability (or rate) of growth depends on the position of the cell relative to the other cells in the growing object. Once a cell is chosen for growth, its direction of growth is then determined with another random number. If all eight directions have equal probability, the growth is isotropic; otherwise, it is anisotropic. Additional conditions involving the number of neighbor cells may be imposed on a cell chosen for growth. Different types of cells may be specified, and the different types may have different growth rules. In this case, the tissue is differentiated. There may also be boundary-smoothing algorithms which suppress random spatial fluctuations along the edges of the tissue.

Programming the growth rules is straightforward. Each cell is assigned an integer number equal to the numerical order of its appearance. Random numbers R, for which $0\le R\le1$, are called to determine the growth process. For an object with N cells, a cell numbered M is chosen for growth according to the rule $M=I(RN)+1$,

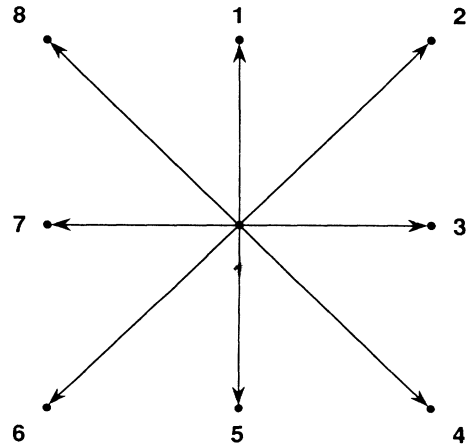

FIG. 1. The numbered growth directions on the square lattice.

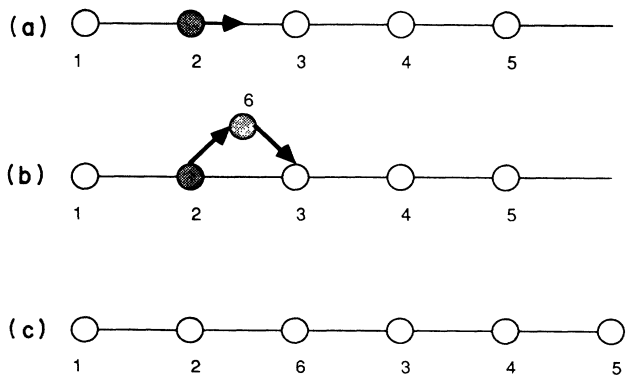

FIG. 2. Illustration of sliding growth in a group of five cells. In (a), cell no. 2 has been chosen for growth to the right. In (b), a daughter cell, no. 6, is created and moved one lattice spacing to the right of cell no. 2. In (c), cells 3, 4, and 5 have been displaced one spacing to the right to make room for the new cell.

where I refers to the integer obtained by truncation of the argument. If the growth is nonuniform, then the growth probability P is computed for the chosen cell and a new random number R' is called. If $0\le R'<P$, then the chosen cell is allowed to grow; if $P\le R'\le1$, then growth is not allowed and the growth cycle is repeated.

Once a cell is chosen for growth, a direction is determined. If the growth is anisotropic, the probabilities $P_1,\ldots,P_8$ must be specified. Then a random number R is chosen and if $0\le R\le P_1$, choose direction 1; if $P_1<R\le P_1+P_2$, choose direction 2; if $P_1+P_2<R\le P_1+P_2+P_3$, choose direction 3; etc. For isotropic growth, all of the P values are equal to 0.125.

Random cellular automata models have the advantage of being easy to program and fast in execution. This allows us to make repeated trials with variable values of growth parameters in the search for agreement with observed biological-growth patterns. The principal disadvantage is that the growth rules are rather abstract and difficult to relate to actual biochemical mechanisms.

III. AREA GROWTH

The simplest two-dimensional growth pattern is uniform, isotropic, undifferentiated growth. The rules for this growth pattern are (1) start with one cell, usually at the center of the box; (2) pick one of the N cells at random; (3) pick one of the eight growth directions at random; (4) insert the new cell [the $(N+1)$st] at the nearest-neighbor position in the growth direction from the chosen cell; and (5) if the new cell overlaps an older cell, move this older cell one space in the growth direction, and continue this displacement process until an empty space is filled.[5] The resulting shape is a circular mass of cells with a rough boundary, as shown in Fig. 3.

This model produces a fractal boundary as in the Eden cluster model[1] because of the random choice of cell and growth direction. In typical biological tissues, such boundary structure is unlikely to occur, because the tissue has a "surface tension" or a plastic yielding behavior

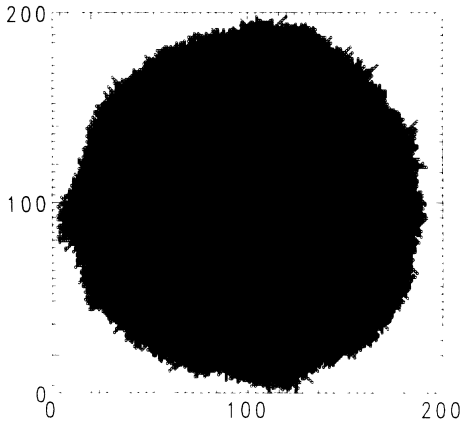

FIG. 3. An example of isotropic and uniform growth without boundary smoothing. The cluster contains 27 000 cells in a 200×200 box.

which spreads out the strain resulting from internal cell growth. We can mimic such boundary smoothing by requiring that the final cell in any sliding displacement must have not fewer than N_b nearest (live) neighbors. If this rule is violated, the move is rejected and a new cell is chosen. If $N_b=1$, then we have the original unsmoothed boundary condition, but if $N_b=2$ or $N_b=3$, then the boundary will be smoothed, as shown in Fig. 4. Sustained growth is not possible for $N_b>3$. Boundary smoothing is a nonlocal growth rule in the sense that the growth of a given cell is determined by conditions distant from that cell.

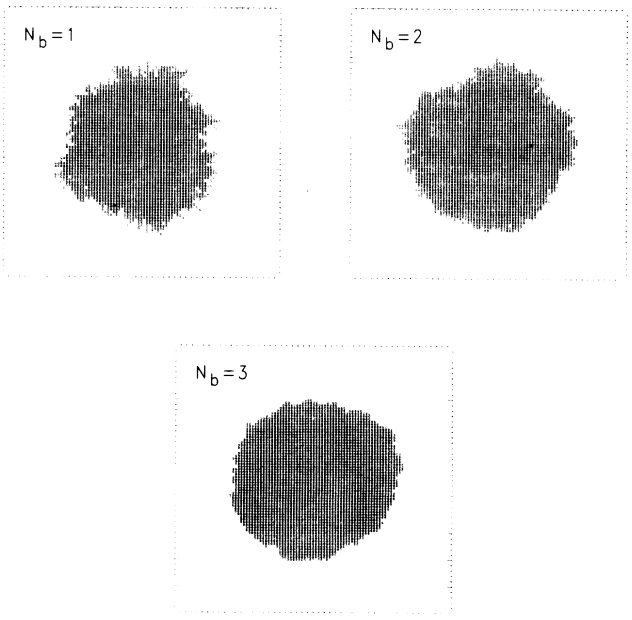

FIG. 4. Isotropic and uniform growth with various values of boundary-smoothing parameter N_b. Each cluster contains about 2500 cells in a 100×100 box.

Nonuniform and anisotropic growth rules may give rise to noncircular shapes. In such cases, we have the counterintuitive result that the shape changes continuously with growth in size.[6] This follows from the various unequal directional growth probabilities or rates, each corresponding to exponential growth with a different exponent. The shape is determined by ratios of exponentially growing dimensions, so that these ratios are themselves changing exponentially. For example, anisotropic growth in which the 1 and 5 directions have higher probabilities than the 3 and 7 directions will give an elliptical shape with a steadily increasing eccentricity. This is shown in Fig. 5.

Nonuniform growth requires that the growth rate or probability be a function of position, $P=P(x,y)$. Here for simplicity we make the growth probability of a cell a function only of its relative position x^* along the x axis:

$$x^*=\frac{x-x_{\min}}{x_{\max}-x_{\min}} \tag{1}$$

and

$$P(x^*)=P_0+(x^*)^k(1-P_0)\ , \tag{2}$$

where $x_{\min}$ and $x_{\max}$ are the boundaries of the growing object in the x direction. The two parameters P_0 and k will determine the degree of nonuniformity of growth. If $P_0=1$ or if $k=0$, the growth rate is uniform. If $P_0=0$, then the growth probability varies over the range 0–1 as x^* varies from 0 to 1. The growth probability in any direction i is $P(x^*)P_i$.

In Fig. 6, we illustrate nonuniform growth. Here the starting configuration is a small rectangular block of cells with three types of differentiated cells. The growth direction is 3 (to the right) only, and the growth probability is given by $P_3=P(x^*)$, as in Eq. (2). Since each cell repro-

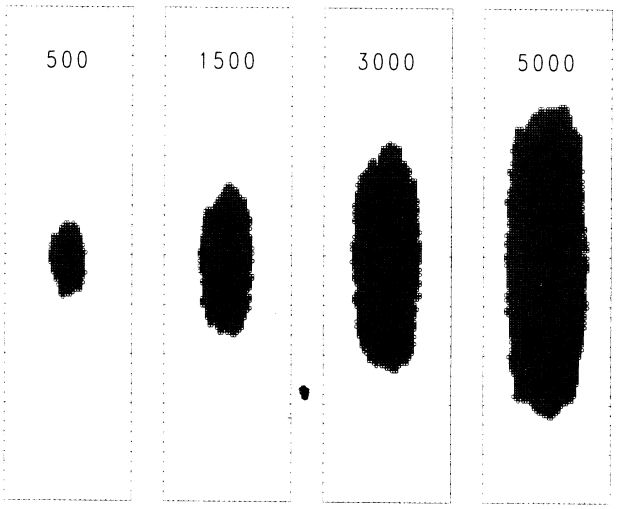

FIG. 5. Anisotropic growth sequence, with $P_1=P_5=0.3333$, $P_3=P_7=0.1667$, and $N_b=3$. The box size is 50×200, and the number of iterations is shown. The elliptical form increases in eccentricity with growth.

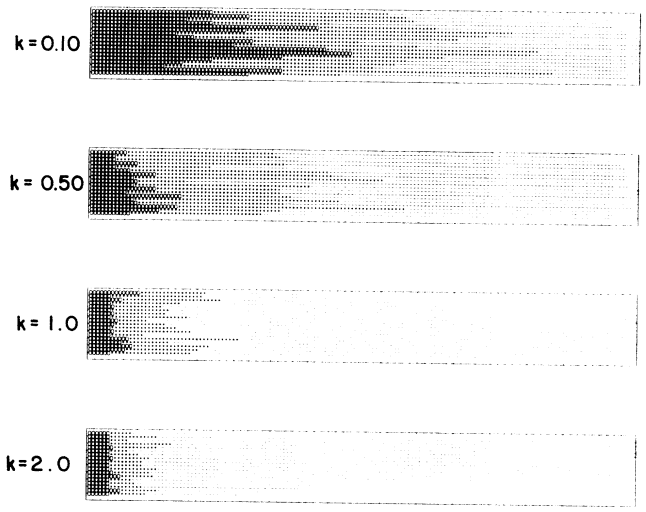

FIG. 6. Nonuniform growth in differentiated cells. Each simulation begins with a 16×18 block of cells containing three cell types, indicated by the three different symbols. The box size is 150×20. The growth is in direction 3 only, and the probability function of Eq. (2) is used, with $P_0=0$. The exponent k is varied in the four simulations to produce different distributions of the three cell types.

duces only its own type, the nonuniformity of the growth pattern can be seen in the relative sizes of the three differentiated regions. In Fig. 6, $P_0=0$, and k is varied to illustrate the spectrum of nonuniform growth distributions. At $k=0.1$, the growth is nearly uniform and the three cell types are nearly equal in number. As k increases beyond this value, the rightmost cell type increasingly dominates the growth. The phenomenon of nonuniform growth for different tissues or organs is very common in biology, and is termed *allometry*.[6]

A specific example of area growth is that of the fern gametophyte. This tiny green plant germinates from a fern spore and develops a characteristic heart shape. We wish to find a growth algorithm which will produce this shape starting from a single cell. By trial and error, we have developed the following rules: (1) start with a single cell at $x=x_0$; (2) for cells at $x=x_0$, allow all growth directions except 1, i.e., $P_1=0$, $P_5=0.3$, $P_i=(i\neq 1,5)=0.1167$; (3) for cells at $x<x_0$, allow only growth directions 1, 5, 6, 7, 8; (4) for cells at $x>x_0$, allow only growth directions 1, 2, 3, 4, 5; and (5) for $x\neq x_0$, vary the directional growth probabilities according to the rules

$$P_1=0.2\left[\frac{|x-x_0|}{30}\right]^k \quad \text{for } |x-x_0|<30\ , \tag{3}$$

$$P_1=0.2 \quad \text{for } |x-x_0|>30\ , \tag{4}$$

$$P_5=0.4-P_1 \quad \text{for all } x\ , \tag{5}$$

and

$$P_i=0.2 \quad \text{for all } i\neq 1,5\ . \tag{6}$$

The arbitrary scale value of 30 in Eq. (3) is chosen to be the approximate size of the organism when growth simulation is stopped. By varying the exponent k, we can control the shape of the "notch" region around $x=x_0$. As shown in Fig. 7, the value $k=0.5$ appears to be the best when compared with an actual gametophyte. The temporal development of the model shape is also in reasonable agreement with observations on the growth of individual gametophytes.[7]

In modeling area growth, our sliding growth models yield results close to the accretion growth models used in physics.[1] The main difference between the two growth models is that sliding growth may be used to generate clones of cells internal to a tissue, while accretion growth cannot. The appropriate physical analogy to area growth might be the growth of a crystalline phase from a liquid or vapor medium. Under uniform external conditions, a growing crystal is likely to take on a compact, symmetric form like a snowflake.[8] By applying temperature or concentration gradients across the growing object, an anisotropic shape like that of Fig. 5 may be produced.

Many examples of biological growth are not random but are more nearly deterministic, in that the cell divisions follow a fixed sequence.[9,10] This is the case in the fern gametophyte, and deterministic models of growth have successfully simulated the growth of this organism.[11] However, we have found that a random growth model constrained by probability functions does an equivalent and adequate job of modeling the growth pattern. We do not have to write into the program a complex set of rules governing sequential cell divisions, but only a simple probability function. A series of simulations with variable k exponent values then generates the patterns, one of which is selected as a best fit to observation.

The anisotropic and nonuniform growth patterns

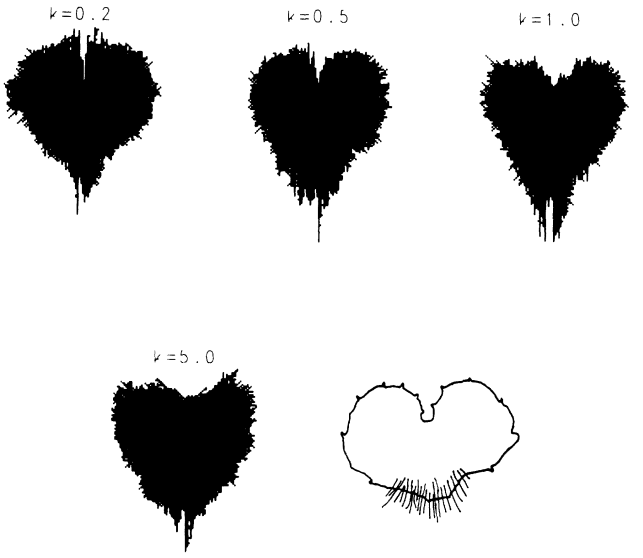

FIG. 7. Simulations of a fern gametophyte with variable anisotropy parameter k. Each simulation contains 5000 cells and $N_b=1$. A sketch of an actual gametophyte is shown also for comparison.

shown in Figs. 5 and 6 illustrate the importance of growth gradients in biological pattern formation.[6] The biochemical mechanisms underlying these gradients are not known, but the standard theoretical model proposes that a gradient of cell behavior is a response to a concentration gradient of a biologically active substance.[12] The spatially varying concentration field constitutes a "morphogenetic field." In the fern gametophyte case, the morphogenetic field might be due to a growth regulator substance originating from the cells at the apical notch. The concentration of the regulator decays with distance, corresponding roughly to the function in Eq. (5).

IV. SHAPE TRANSFORMATIONS

In his book *On Growth and Form*, D'Arcy Thompson proposed that closely related organisms should be compared quantitatively by a point-to-point mapping of one onto the other.[13] He illustrated this by drawing a rectangular grid over one of the organisms and an appropriately distorted grid over the other. This diagram (Figs. 8 and 9) suggests how to "transform" one organism into another by differential growth. These transformations are smooth and are the same for all of the various differentiated tissues found in the organisms being compared.

Thompson's grids have been admired and commented on for decades, but they have not proved to be of practical use to biologists.[14] The problem is that the grid transformations are not constant, but depend on the size of the organisms being compared. This follows from the rule that anisotropic or nonuniform growth produces a shape which constantly changes with increase in size, as indicated in Figs. 5 and 6.

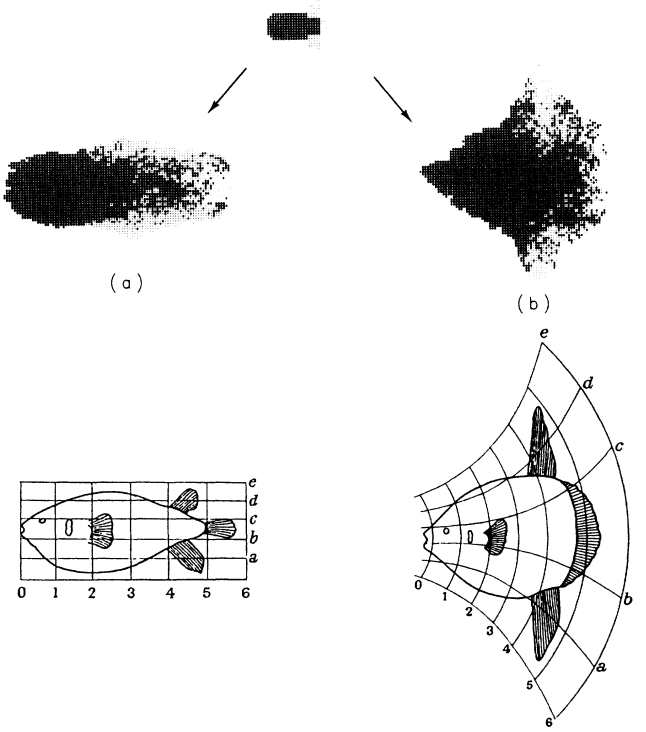

FIG. 8. Simulation of one of Thompson's coordinate transformations for two fish species. The upper figure is an "embryo" initial condition for both simulations, which contains three types of cells. Anisotropic growth rules with $N_b=3$ are applied to the embryo, leading to the two forms designed to mimic the fish species drawn below with their coordinate transformation. Simulation (a) is generated with $A=B=0.35$, and simulation (b) is generated with $A=0.1$, $B=1.0$, and $k=1.0$. (Lower figures are reprinted with permission from Ref. 13.)

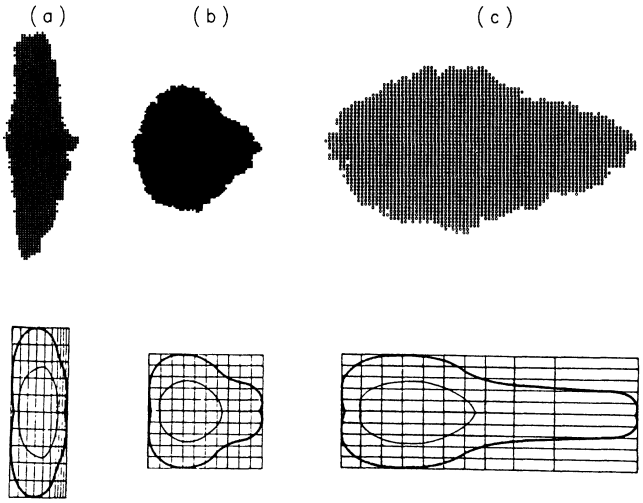

FIG. 9. Simulations of cucurbit fruit forms using anisotropic growth model with $N_b=3$. The coordinate transformations are drawn below. Simulation (a) is generated with $A=1.0$, $B=0$, and $k=2.0$. Simulation (b) is generated with $A=0.95$, $B=0$, and $k=1.0$. Simulation (c) is generated with $A=1.0$, $B=0$, and $k=0.6$ (Lower figures are reprinted with permission from Ref. 15.)

A more fundamental comparison of two organisms would be between the two growth algorithms which govern their shapes. These algorithms are more likely to remain constant over a range of sizes than the shapes of the organisms. We can use our simulation technique to determine the algorithms for two species of tropical fish considered by Thompson, and shown in Fig. 8. The two species differ in the ratio of head to tail size.

The anisotropy is given a spatial dependence in order to provide more realistic simulations. In these calculations we restrict the growth directions to 1, 3, 5 and 7, with

$$P_1=P_5=0.5[A+(x^*)^k(B-A)]\,, \tag{7}$$

and

$$P_3=P_7=0.5(1-2P_1)\,, \tag{8}$$

where $0\le A,\ B\le 1$. The general nonuniform growth probability of Eq. (2) is also included in the simulation.

We start with an "embryo" containing differentiated tissues and we apply different growth rules in order to obtain the two adult fish shapes. The "control" shape is obtained approximately with constant anisotropy, $A=B=0.35$. This represents growth which is biased in the 3 and 7 directions. The "distorted" shape requires increased vertical growth in the tail region. Our best simulation is obtained with $A=0.1$, $B=1.0$, and $k=1.0$. We

do not need to invoke nonuniform growth for these simulations. Although our model cannot prevent the unrealistic intermixing of different cell types, the simulated shapes of the body and tail fins are in reasonable agreement with the observed shapes. Since these two fish species are closely related, it is possible to imagine an ancestral species which underwent divergent evolution by stepwise change in the genes controlling the growth probabilities of its tissues. The specific mechanisms controlling the growth probabilities are not known, but a morphogenetic field model is plausible.

An example of shape variation among plants is found in the fruits of cucurbits (squashes and gourds). These have been studied with Thompson's grids and are also found to have smooth grid transformations.[15] We have simulated these shapes using Eqs. (7) and (8), starting from a very simple rectangular embryo, and the results are shown in Fig. 9. As with the shapes of Fig. 8, it was not necessary to apply nonuniform growth.

Here we have specified simple algorithms for the production of varied biological shapes. The algorithms are more fundamental than the shapes, which change as a function of size. In confirmation of this, experimental genetic studies of the cucurbit shapes show that it is the growth rates and directions which are hereditary, and not the shapes themselves.[15]

The rather crude shapes of the simulations in Figs. 8 and 9 are the result of the very simple model with a limited number of adjustable parameters. More elaborate models with more parameters could certainly produce better fits to observations, but this is unnecessary for illustrating the principle of the growth model.

V. BRANCHING GROWTH

Some organic structures like fungi, plant roots, and blood vessels have a threadlike, branching growth habit. Here the important growth rules have to do with the elongation of the threads and the rate and direction of branching.

Here we apply the lattice model to branching growth in two dimensions. For a lattice of points in two dimensions, we consider a set of growth rules: (1) start with a single cell; (2) choose a cell at random; (3) choose a growth direction with a random number according to the assigned probabilities; (4) check to see if the new site is unoccupied and that it meets neighbor number criteria; (5) if the criteria are met, then place the new cell at the specified position and connect it to its origin with a straight line.

These rules generate a set of connected line segments. For branching growth, we may assume that the purpose of the growth is to fill space in an optimal way in order to absorb nutrients distributed in space or to provide nutrition to other tissue distributed in space. To do this, the branches must avoid one another and growing tips must orient away from one another. This can be done by requiring that any prospective cell must not have more than some number N_c of neighbor cells. The simplest rule specifies nearest neighbors only, but second- and higher-neighbor numbers can be introduced easily. The growth in this case is not sliding growth but accretion growth, in which cells are placed at unoccupied points on the lattice. In Fig. 10, we show the results of isotropic branching growth for nearest-neighbor number $N_c = 1$, 2, 3, and 5.

The patterns shown in Fig. 10 do not accurately mimic observed growth patterns because real branching growth is generally not isotropic.[16] Anisotropic growth occurs because this is the most efficient way to occupy new space. In modeling this, the probability of growth direction can be "biased" by giving more weight to certain favored directions. In a radially growing fungus colony, there is a bias in the direction radially outward from the original cell, because this is where the nutrients are.

A radial bias may be introduced by redefining the directional probabilities $P_1, \ldots, P_8$. At the position of the chosen cell, the radial direction is defined as direction 1 and is given probability P_1. The seven other directions are arranged with respect to this direction as in Fig. 1 and assigned probabilities $P_2, \ldots, P_8$. To translate a randomly chosen direction into one of the eight allowable directions on the lattice, we compute the tangent of the angle θ formed by the chosen direction and the x axis, and compare this with the tangents of the angles α_i corresponding to the eight allowable directions. If $\tan\theta$ lies between $\tan(\alpha_i + \pi/8)$ and $\tan(\alpha_i - \pi/8)$, then the growth direction is i.

In the case of fungal colonies, the radially outward direction may be favored, and in Fig. 11, this type of growth is shown for variable radial growth bias parameter, as indicated by the P_1 value. Here only the radially outward growth directions 1, 2, 3, 7, and 8 are allowed.

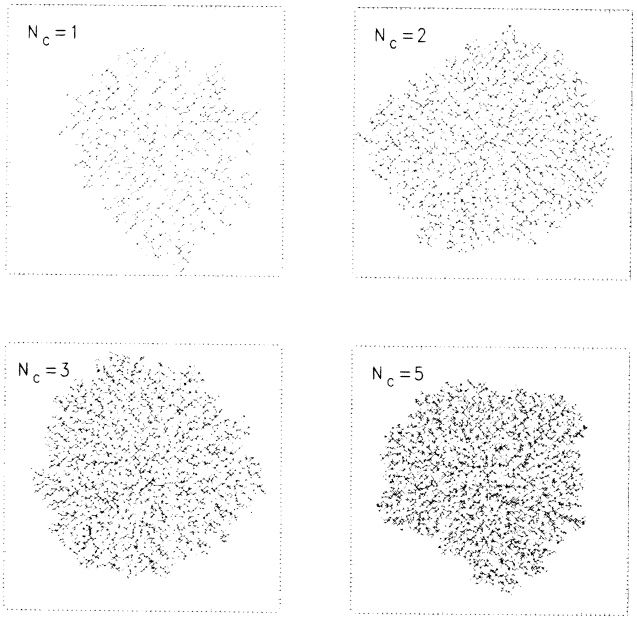

FIG. 10. Isotropic branching growth with variable nearest-neighbor rule. The box size is 100×100 and the N_c values are shown.

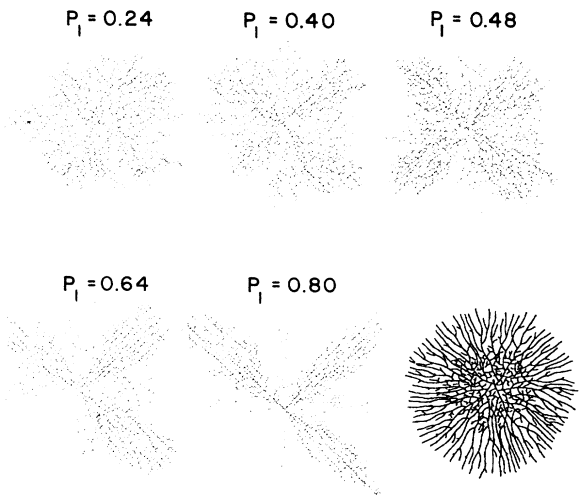

FIG. 11. Branching growth with radial anisotropy. The P_1 value is shown above each simulation. Here $P_2=P_3=P_7=P_8=0.25(1-P_1)$. A sketch of an actual fungus colony is shown in the lower right corner.

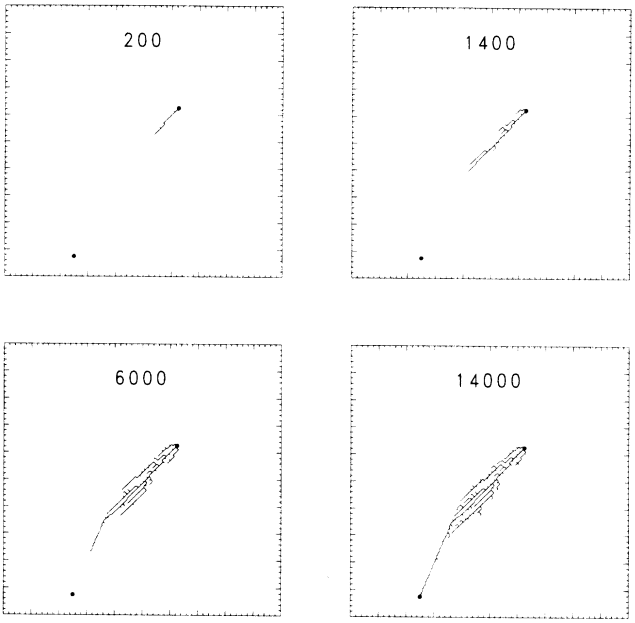

FIG. 12. Growth of a branching structure toward a point source in a 100×100 box. Here $P_1=0.96$, and $P_2=P_3=P_7=P_8=0.01$. The iteration of each growth stage is shown.

The simulations with higher P_1 values are in moderately good agreement with a sketch of a fungal colony also shown in Fig. 11. The simulated colonies are space-filling structures which have a fractal dimension D. The number D may be determined from the slope of a log-log plot of the number of cells in the colony versus the average linear dimension of the colony. Unbiased colonies fill space uniformly and have a fractal dimension $D=2$. With increasing radial bias, branching is suppressed, the structure becomes increasingly one-dimensional, and D approaches 1. Although branching growth is probably nonuniform as well as anisotropic, for the sake of simplicity we have not included nonuniformity.

Growth can also be biased toward a point source of nutrient. This is done by specifying the favored growth direction 1 in the direction of the point source and by using the tangent method as before. An example of strongly biased growth in the direction of a point source is shown in Fig. 12. This resembles the growth of fungal filaments toward a nutrient source or the growth of a neuron toward a target cell in animal tissue.

Branching growth in biology has numerous physical analogies, including diffusion-limited aggregation (DLA), electrodeposition, viscous fingering, and electric discharges.[1,2,4,17] In two-dimensional space, these physical growth processes lead to objects of fractal dimension D, with $1<D<2$, not unlike the branched structures of Fig. 11. The DLA model introduces an inherent radial growth bias by virtue of its boundary conditions, but this bias has been specifically introduced as a "tip priority factor" in modeling the electric breakdown of insulators.[17]

The fractal dimension of a biological-growth pattern is unfortunately not very informative about the important growth mechanisms, which include cell elongation and branching. Studies of these processes in fungi suggest a complex process of cell wall breakdown and synthesis.[18] Slight changes in this process due to mutation may lead to significant changes in the shapes of colonies and in the adaptive efficiency of the organism. The usefulness of the models lies in making the connection between the microgrowth processes and the macrocolony form.

VI. LEAF GROWTH

The innumerable variety of leaf forms presents a formidable challenge to theoretical biology. In modeling leaf growth, we look for growth rules which are simple, but which contain sufficient variability in parameter space that a variety of forms may be generated from iteration of the rules. In leaves, the growth pattern is more complex than either simple area or branching growth. In fact, we model it as a combination of both types. We consider two types of cells, vein cells and green photosynthetic cells. The branching vein cells grow by converting green cells, and the green cells fill space by accretion. Green cells can grow only if they are sufficiently close to vein cells, which supply nutrient. Thus there is a positive feedback linking the growth of the two types of cells.

Specification of the probabilities of growth and growth direction of the two types of cell allows for an elaborate set of rules which may be sufficient to simulate the great variety of growth patterns found among leaves. Here, however, we confine ourselves to very simple rules in order to provide a minimal description of one generic leaf type, the oak leaf.

For vein cells, the rules are (1) start with an embryo with one vein cell; (2) this cell grows upward to form the

midrib by converting green cells; (3) if a green cell directly above the top of the midrib has at least N_v other live neighbors, then it is converted to a new midrib vein cell; (4) initiate horizontally growing secondary veins at constant intervals y_n along the midrib; and (5) secondary veins grow when a random number selects a vein tip, and the neighboring green cell in the direction of growth has at least N_v live neighbors. In order to keep the model simple, we have neglected the formation of tertiary and higher-order veins.

For green cells, the rules are (1) start with an embryo containing several green cells; (2) pick a green cell at random; (3) pick a growth direction according to the assigned probabilities; and (4) if the prospective cell position is unoccupied, and if it is within n_s shells of neighbors of the nearest vein cell, allow growth by accretion.

By varying the numbers y_n and n_s, the outline of the leaf can be made to vary from highly lobed or dissected to roughly circular. These simulations are shown in Fig. 13 and are compared with leaves of several California oak species. The agreement is moderately good.

Since the oaks belong to the same genus and are closely related, it follows that the leaf shapes should be the result of only slight variations on a general growth pattern. This is consistent with our approach in varying only a few parameters to obtain the observed shapes.

There is an interesting analogy between the leaf model and river drainage basins as studied in physical geography.[19] The patterns of channels and drainage area correspond to the veins and green tissue, respectively. As water drains into the river, the stream channels deepen and the network of channels becomes more elaborate. This is equivalent to the elaboration of the vein network in leaf growth. Theoretical work on vein formation in leaves suggests that veins form in response to flows of auxin,[20] a growth regulator, which is analogous to water flows stimulating the formation of stream channels. There is also an analogy between the growth of dendritic crystals and of leaves, not only in shape, but in the sensitivity of the shape to the boundary conditions.[8,21]

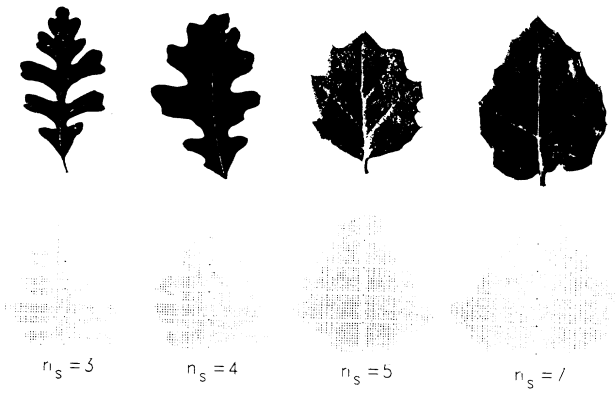

FIG. 13. Simulations of oak leaf patterns. Actual leaves with varying degrees of dissection are compared with best simulations using $N_v = 8$, $y_n = 12$, and variable neighbor shell numbers n_s.

VII. DISCUSSION

Biological growth touches the problems of physical pattern formation processes at various points, and there are a number of rather close analogies between the two, which suggests fundamental topological similarities.[4,13,22] This has been useful in applying cellular automata models to biological-growth problems. Unlike physics, however, the immense complexity of biophysical phenomena makes attempts at exact simulation and mathematical analysis unrewarding. Instead, we strive to generate the simplest model which captures the essential features of the observed phenomenon.

Lattice models have the valuable property of simplicity and ease of programming. Thus they can be used to simulate complex structures by a trial-and-error process of adjusting the generating algorithm until the desired structure is obtained. We have found that intuition rarely gets the right answer at the first trial, since the iterative process of simulation is too difficult to predict. The trial-and-error process aids in converging to the correct algorithm, and is an essential part of the research effort.

It is also possible to generate increasingly complex rules for lattice models if there are sufficient quantitative experimental data to warrant this. An example might be Sinnott's extensive genetic work on cucurbit shapes.[15] It would be straightforward to generalize the lattice model to three dimensions, and three-dimensional growth rules which accurately mimicked cucurbit growth patterns might suggest further experimental work to study the anisotropic growth rules at the cellular level.

In this paper, we have made only general suggestions about mechanisms at the genetic level because very little is known about these mechanisms. However, accurate modeling of growth and the stating of explicit rules opens the way to new theoretical and experimental work on biochemical mechanisms. Lattice models may thus have a valuable contribution to make in addressing problems of biological morphogenesis, variation, and evolution.

ACKNOWLEDGMENTS

This work was performed under the auspices of the U.S. Department of Energy by Lawrence Livermore National Laboratory under Contract No. W-7405-Eng-48. We thank R. Minich for a valuable critique of the manuscript.

[1]T. Vicsek, *Fractal Growth Phenomena* (World Scientific, Singapore, 1989).

[2]P. Meakin, in *Phase Transitions and Critical Phenomena,* edited by C. Domb and J. L. Lebowitz (Academic, London, 1988), Vol. 12, p. 336.

[3]*Random Fluctuations and Pattern Growth: Experiments and Models,* edited by H. E. Stanley and N. Ostrowsky (Kluwer Academic, Dordrecht, 1988).

[4]P. Meakin, J. Theor. Biol. **118**, 101 (1986).
[5]R. Ransom, *Computers and Embryos* (Wiley, Chichester, 1981), Chap. 7; P. M. Iannaccone, L. Berkwits, J. Joglar, L. Lindsay, and A. Lunde, J. Theor. Biol. **141**, 363 (1989).
[6]J. S. Huxley, *Problems of Relative Growth* (Dover, New York, 1972) (reprint of 1932 edition).
[7]R. O. Erickson, in *Automata, Languages, Development,* edited by A. Lindenmayer and G. Rozenberg (North-Holland, Amsterdam, 1976), p. 39.
[8]J. Nittman and H. E. Stanley, J. Phys. A **20**, L1185 (1987).
[9]A. Lindenmayer, in *Developmental Order: Its Origin, and Regulation,* edited by S. Subtelny and P. B. Green (Liss, New York, 1982), p. 219.
[10]A. Lindenmayer and P. Prusinkiewicz, in *Artificial Life,* edited by C. G. Langton (Addison-Wesley, Redwood City, 1989), p. 221.
[11]R. W. Korn, Bot. J. Linn. Soc. **68**, 163 (1974).
[12]H. Meinhardt, *Models of Biological Pattern Formation* (Academic, London, 1982).
[13]D. W. Thompson, *On Growth and Form* (Cambridge University Press, Cambridge, 1966) (abridged edition).
[14]F. L. Bookstein, Math. Biosci. **34**, 177 (1977).
[15]E. W. Sinnott, *The Problem of Organic Form* (Yale University Press, New Haven, 1963), Chaps. 2. and 6.
[16]A. D. Bell, Philos. Trans. R. Soc. London, Ser. B **313**, 143 (1986).
[17]Y. Sawada, S. Ohta, M. Yamazaki, and H. Honjo, Phys. Rev. A **26**, 3557 (1982).
[18]*The Filamentous Fungi. Developmental Mycology,* edited by J. E. Smith and D. R. Berry (Wiley, New York, 1978).
[19]P. Haggett and R. J. Chorley, *Network Analysis in Geography* (St. Martin's Press, New York, 1970), Chap. 2.
[20]G. J. Mitchison, Philos. Trans. R. Soc. London, Ser. B **295**, 461 (1981).
[21]J. Kertesz, in *Random Fluctuations and Pattern Growth: Experiments and Models,* edited by H. E. Stanley and N. Ostrowsky (Kluwer Academic, Dordrecht, 1988), p. 42.
[22]P. S. Stevens, *Patterns in Nature* (Little, Brown, Boston, 1974).

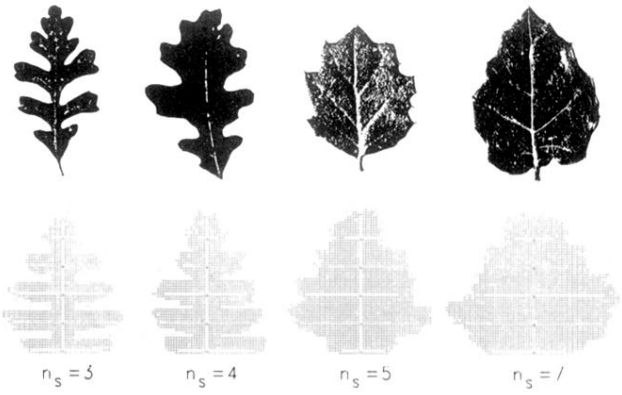

FIG. 13. Simulations of oak leaf patterns. Actual leaves with varying degrees of dissection are compared with best simulations using $N_v = 8$, $y_n = 12$, and variable neighbor shell numbers n_s.

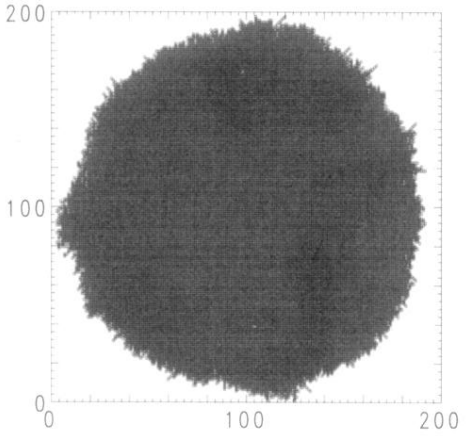

FIG. 3. An example of isotropic and uniform growth without boundary smoothing. The cluster contains 27 000 cells in a 200×200 box.

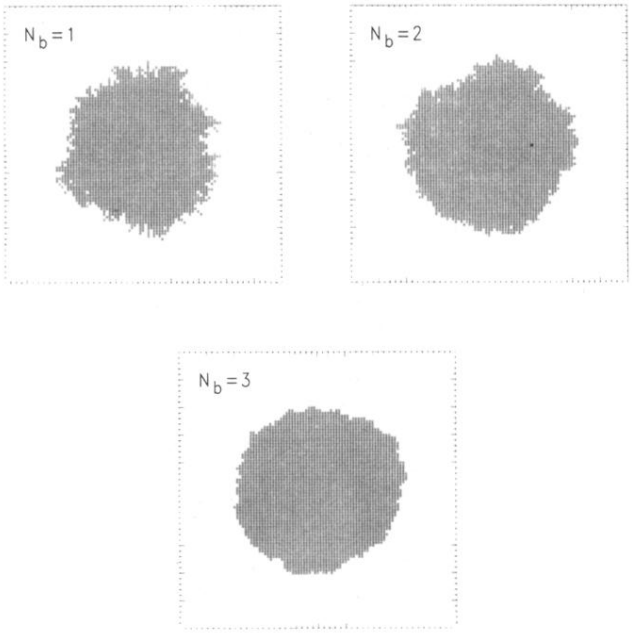

FIG. 4. Isotropic and uniform growth with various values of boundary-smoothing parameter N_b. Each cluster contains about 2500 cells in a 100×100 box.

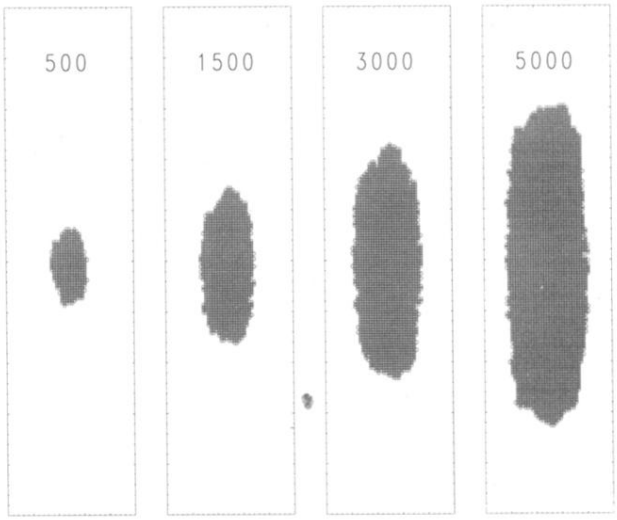

FIG. 5. Anisotropic growth sequence, with $P_1 = P_5 = 0.3333$, $P_3 = P_7 = 0.1667$, and $N_b = 3$. The box size is 50×200, and the number of iterations is shown. The elliptical form increases in eccentricity with growth.

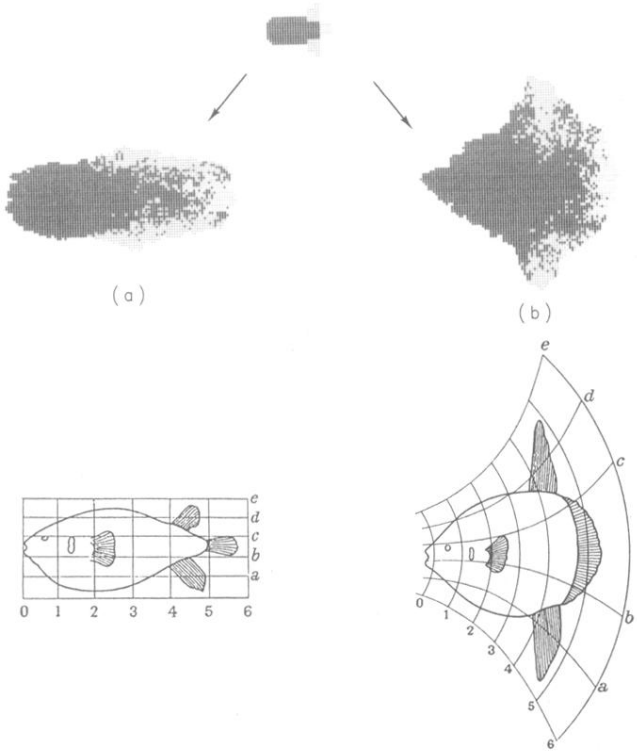

FIG. 8. Simulation of one of Thompson's coordinate transformations for two fish species. The upper figure is an "embryo" initial condition for both simulations, which contains three types of cells. Anisotropic growth rules with $N_b = 3$ are applied to the embryo, leading to the two forms designed to mimic the fish species drawn below with their coordinate transformation. Simulation (a) is generated with $A = B = 0.35$, and simulation (b) is generated with $A = 0.1$, $B = 1.0$, and $k = 1.0$. (Lower figures are reprinted with permission from Ref. 13.)

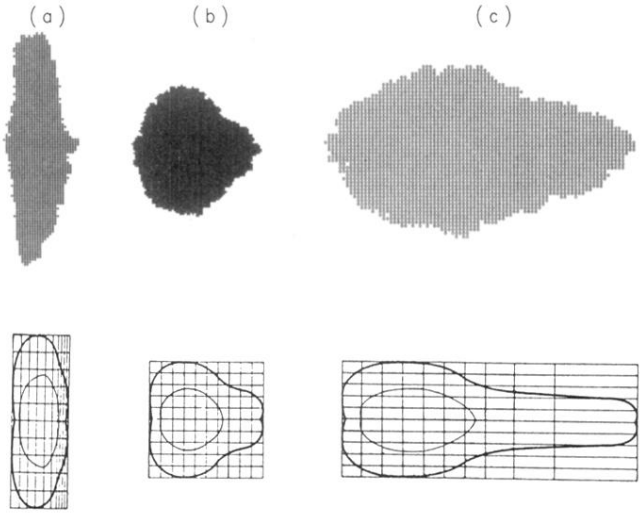

FIG. 9. Simulations of cucurbit fruit forms using anisotropic growth model with $N_b = 3$. The coordinate transformations are drawn below. Simulation (a) is generated with $A = 1.0$, $B = 0$, and $k = 2.0$. Simulation (b) is generated with $A = 0.95$, $B = 0$, and $k = 1.0$. Simulation (c) is generated with $A = 1.0$, $B = 0$, and $k = 0.6$ (Lower figures are reprinted with permission from Ref. 15.)